CHAPTER 9

PROBABILISTIC ANALYSIS OF A CHAOTIC DYNAMICAL SYSTEM

SOLOMON C. S. YIM and HUAN LIN
Department of Civil Engineering
Oregon State University
Corvallis, OR 97331-2302

This study examines the chaotic behavior of a practical nonlinear dynamical system from the perspective of probability-based fatigue design. The stochastic characteristics of chaotic response of freestanding rigid objects subjected to horizontal harmonic base excitations are investigated. An approximate method based on the Melnikov function to predict analytically the existence of chaotic response is presented. Although the excitations to the rocking systems are simple and purely deterministic, some stochastic characteristics of the chaotic responses are detected using Poincaré maps and amplitude probability densities. It is found that although the chaotic time histories have a periodic time dependency (thus nonstationary), time series consisting of Poincaré points may be ergodic. These stochastic characteristics are useful in determining the fatigue life of nonlinear dynamical systems that operate frequently in chaotic states.

9.1. INTRODUCTION

The existence of chaotic response has been observed in many deterministic nonlinear physical and engineering systems [8, 6]. For some systems, the occurrence of chaotic responses is undesirable and should be avoided. However, for other systems, such as mixing of fluids and the control of heart rate variability, the occurrence of chaos may be desirable and should be promoted. In the design of such systems, the effects of long-duration steady-

Applied Chaos, Edited by Jong Hyun Kim and John Stringer.
ISBN 0-471-54453-1

state chaos on fatigue should be taken into account. Because many conventional fatigue design procedures are probability-based, it is important to determine whether chaotic responses possess stochastic properties commonly used in the design procedures. In particular, it is advantageous to examine the stochastic properties of chaotic responses, if they exist, in terms of probability density functions, even though chaotic responses are fully deterministic and repeatable. To demonstrate the stochastic characteristics of chaotic responses, a simple, freestanding rocking system is examined in this study.

The rocking behavior of rigid objects has been of interest to civil engineers for over a century. Many structures, from ancient historical minarets, monumental columns, and tombstones, to modern-day petroleum storage tanks, water towers, power transformers, nuclear reactors, and concrete radiation shields, can be considered to be freestanding objects. They may be subjected to support excitations due to earthquake ground motion and/or nearby machine vibrations. An understanding of the rocking behavior of these objects is of vital importance for safe operations, preservation of existence, and the design of new equipment.

Recent studies have demonstrated that the rocking response of rigid objects can be very sensitive to the system parameters and the excitation details. In a series of dynamic tests performed on the Berkeley shaking table, Aslam, Godden, and Scalise [1] showed that the rocking response was so sensitive that some of the experiments were deemed nonrepeatable. Using a single-degree-of-freedom (SDOF) model for the system, Yim, Chopra, and Penzien [13] examined the sensitivity of the rocking response by conducting a numerical study to identify, in a statistical sense, the parametric dependency of overturning stability on the size, slenderness ratio, coefficient of restitution, and ground motion intensity. The deterministic results confirmed that the rocking response can be sensitive to small changes in system parameters, and probabilistic trends can be established only with a large sample size.

Recognizing the insurmountable difficulties in the analysis of the complex behavior of the fully nonlinear rocking objects subjected to earthquake excitations, Spanos and Koh [7] and Tso and Wong [9] simplified the SDOF system by assuming the rigid objects to be slender and the base excitation to be harmonic, thus allowing linearization of the individual governing equations of motion and removing the randomness in the excitation. They were able to develop approximate analytical methods to predict the existence and stability of harmonic and subharmonic responses. Hogan [3] extended the stability analysis methods and developed a procedure to predict the existence of chaotic responses. He applied his prediction procedure to analyzing the experimental data of Wong and Tso [11] and was able to obtain a quantitative match. As a result of these studies, significant advances in the understanding of the rocking behavior were made.

Recently, Yang and Cheng [12] discovered new features of chaotic responses of nonlinear systems that fall in between the typical deterministic

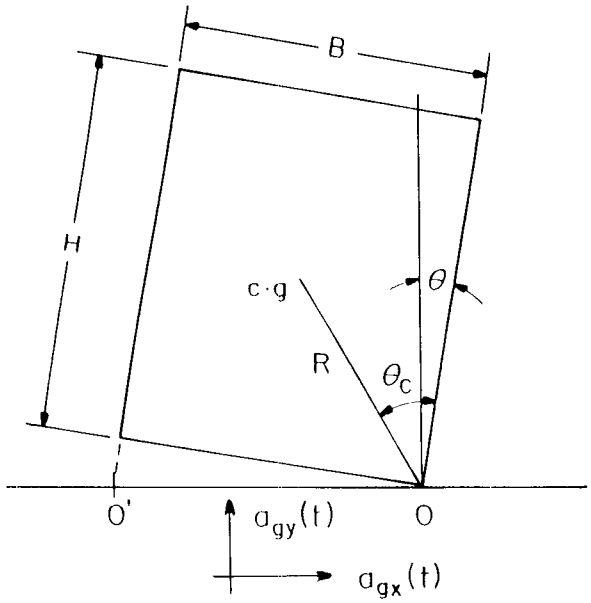

Figure 9.1. Freestanding rigid rocking object subjected to horizontal and vertical excitations.

and stochastic dynamics. They showed that, in a stochastic sense, the steady-state chaotic process is stationary and ergodic in terms of Poincaré time series. Kapitaniak [5] also developed a new indicator of chaotic response in a probabilistic sense. He pointed out that the chaotic response has a multimaxima curve in the amplitude probability density function.

This investigation focuses on identifying possible stochastic properties of chaotic responses of the simplified system. An approximate analytical method based on the Melnikov function to predict the existence of chaotic responses is first derived. The analysis techniques developed by Kapitaniak [5] and Yang and Cheng [12] are extended and employed to examine their stochastic properties.

9.2. SYSTEMS CONSIDERED

The freestanding slender object is modeled as a rectangular rigid body subjected to horizontal base motion excitation (Figure 9.1). Assuming that the coefficient of friction is sufficient that there will be no sliding between the object and the base, depending on the support accelerations, the object may move rigidly with the base or be set into rocking. If rocking occurs, it is

assumed that the body will oscillate rigidly about the centers of rotation O and O'. The governing equation of motion for the rigid object with positive angular rotation about corner O is [13]

$$I_O\ddot{\theta} + MRa_{gx} + MgR(\theta_{cr} - \theta) = 0, \qquad \theta > 0 \tag{9.1a}$$

where I_O is moment of inertia about O, M is mass, a_{gx} is the horizontal base acceleration, R is the distance from O to the center of mass, and $\theta_{cr} = \cot^{-1}(H/B)$ is the critical angle beyond which overturning will occur for the object under gravity alone (H and B are the height and width of the object). Similarly, the rocking about O' is governed by the equation

$$I_O\ddot{\theta} + MRa_{gx} - MgR(\theta_{cr} + \theta) = 0, \qquad \theta < 0 \tag{9.1b}$$

Impact occurs when the angular rotation crosses zero approaching from either positive or negative, and the base surfaces recontact. Associated with the impact is a transition from rocking about one corner to rocking about the other and a finite amount of energy loss (or "damping") that can be accounted for by reducing the angular velocity of the object after impact. As in reference [13], it is assumed that the angular velocity before and after impact is related by a parameter e through the following equation:

$$\dot{\theta}(t^+) = e\dot{\theta}(t^-), \qquad 0 \le e \le 1 \tag{9.2}$$

where e is the coefficient of restitution, t^+ is the time just after impact, and t^- is the time just before impact. In this study, the horizontal base excitation is assumed to be harmonic with constant amplitude and a single frequency,

$$a_{gx} = a_x \cos(\omega t + \phi) \tag{9.3}$$

Note that there are two nonlinearities in the system associated with impact. The first results from the transition from one governing equation to the other as the center of rotation changes from one edge to the other. The second is due to the abrupt reduction (jump discontinuity) in the angular velocity caused by the impact (damping). In the limiting case, the damping nonlinearity can be removed if it is assumed that the material of the rigid object and the base support are stiff and that the rebound following impact is perfectly elastic so that there is no energy loss, that is, $e = 1$ (a conservative, or Hamiltonian, system).

9.3. METHOD OF ANALYSIS

Because the individual equations governing the rocking motion about each edge [equations (9.1a) and (9.1b)] are linear, exact analytical solutions for

these equations exist and are used in conjunction with the nonlinear transition conditions at impact in determining the responses [7]. Let $\tau = \alpha t$ and $\Omega = \omega/\alpha$ [where $\alpha = (MgR/I_O)^{1/2}$] be the normalized time and frequency, respectively, the piecewise linear versions of (9.1a) and (9.1b) can be reduced to

$$\ddot{\Theta} - \Theta = \begin{cases} -A_x \cos(\Omega\tau + \phi) - 1, & \Theta > 0 \quad (9.4a) \\ -A_x \cos(\Omega\tau + \phi) + 1, & \Theta < 0 \quad (9.4b) \end{cases}$$

The solutions of (9.4a) and (9.4b) are

$$\Theta^+(\tau) = a^+ \sinh\tau + b^+ \cosh\tau + 1 + \beta\cos(\Omega\tau + \phi) \quad (9.5a)$$

$$\Theta^-(\tau) = a^- \sinh\tau + b^- \cosh\tau - 1 + \beta\cos(\Omega\tau + \phi) \quad (9.5b)$$

The superscript "+" indicates that the expression is valid for $\Theta > 0$ and the superscript "−" indicates that the expression is valid for $\Theta < 0$. The symbols a^+, b^+, a^-, and b^- denote constants of integration dependent on the initial conditions, and $\beta = A_x/(1 + \Omega^2)$. The response to harmonic excitations can be obtained by selecting the proper equation with the appropriate initial conditions and increasing the time variable successively. If at a particular time the magnitude of Θ exceeds 1.0 and continues to diverge, the rigid object will overturn. If Θ returns to zero, then the corresponding angular velocity can be determined and the solution given by the other equation can be applied. This procedure is then repeated until steady-state response is obtained.

9.4. CLASSIFICATION OF RESPONSES

When subjected to harmonic horizontal base excitation, depending on the amplitude and frequency of the excitation, the response of a slender object may either be *unbounded*, which leads to overturning, or it will eventually settle into a *bounded* motion. It has been shown that in addition to *periodic* response, there exist two additional types of bounded responses, namely, *quasiperiodic* and *chaotic* [4, 14]. Examples of these responses are shown in Figures 9.2, 9.3, and 9.4, respectively. In order to determine the regions of existence of chaotic responses, we derive analytical expressions of their boundaries.

9.5. CONDITIONS FOR EXISTENCE OF CHAOTIC RESPONSE

The existence conditions for chaotic response of the rocking system are derived following the methodology outlined by Melnikov [2], and the Melnikov integral function, which includes the effects of nonlinearity and excitations, is

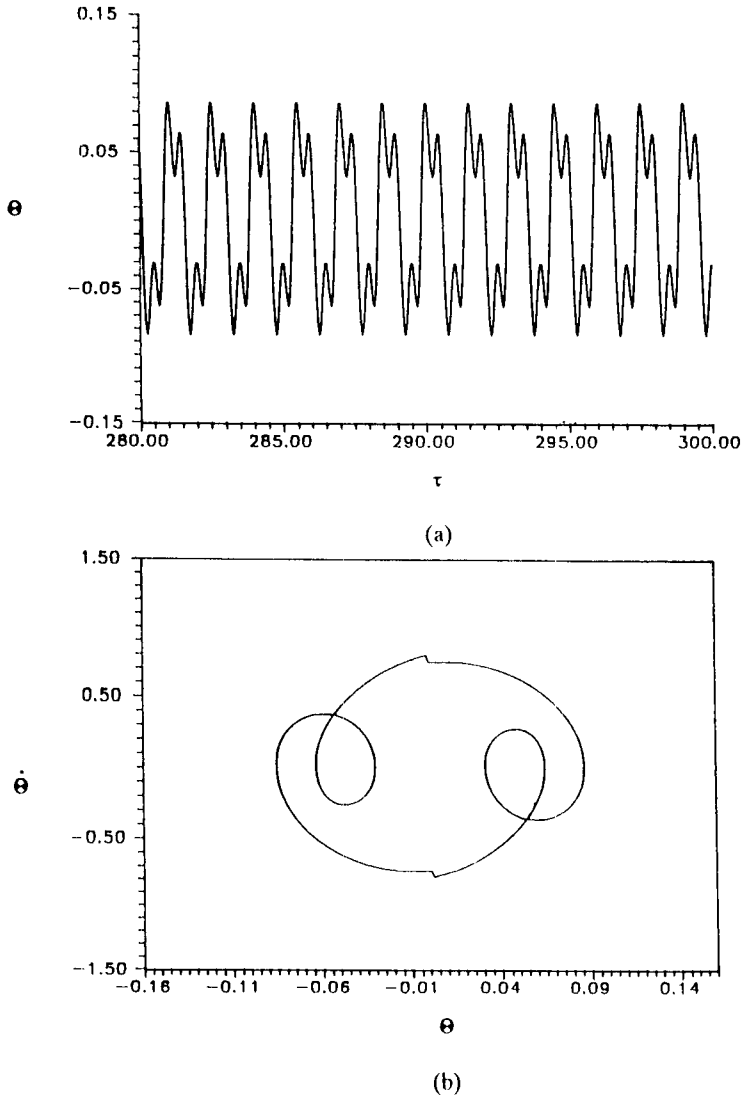

Figure 9.2. Periodic response: (*a*) time history; (*b*) phase diagram.

constructed. The integration is along a closed curve formed by heteroclinic orbits that are trajectories connecting two fixed points. The heteroclinic orbits are identified by examining the phase diagram of the associated (undamped, unforced) Hamiltonian system. Existence of zeros of the Melnikov function indicates the existence of chaotic response. The derivation of the existence conditions is shown as follows.

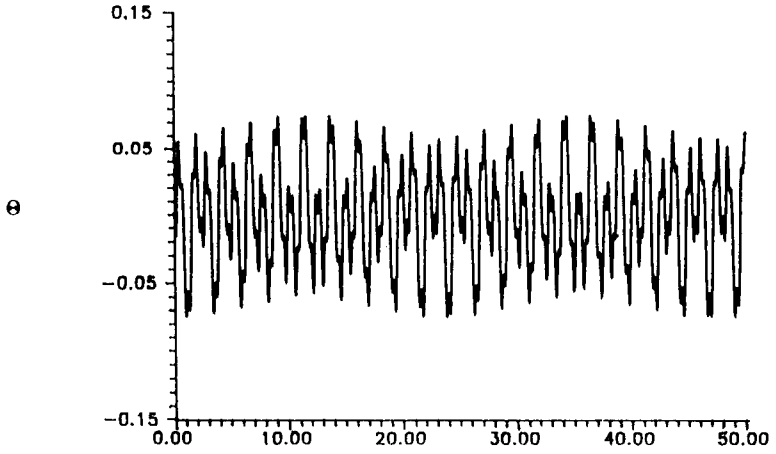

(a)

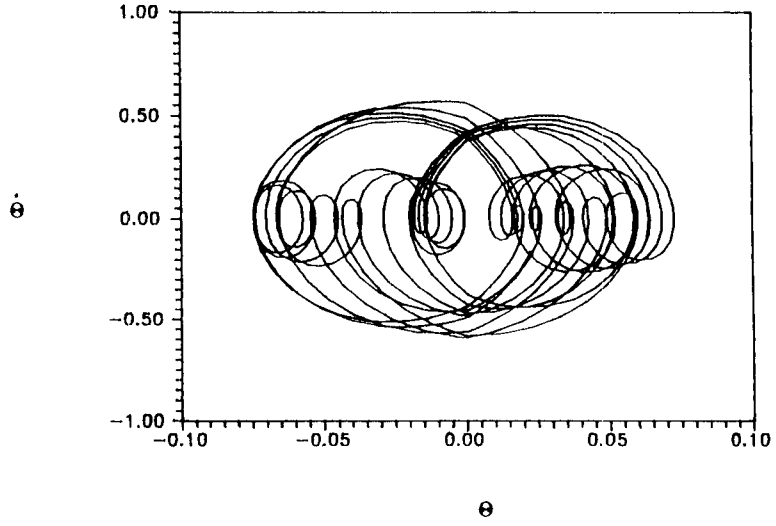

(b)

Figure 9.3. Quasiperiodic response: (*a*) time history; (*b*) phase diagram.

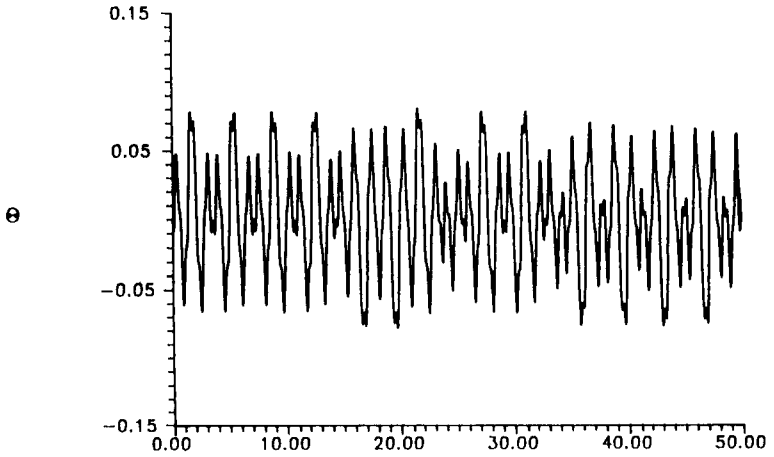

(a)

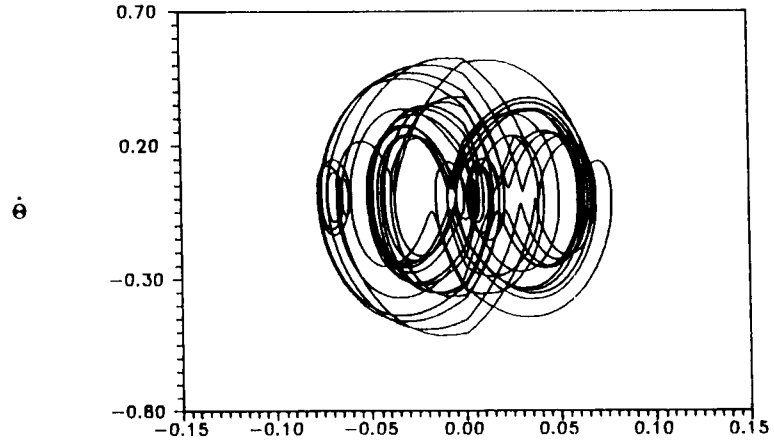

(b)

Figure 9.4. Chaotic response: (*a*) time history; (*b*) phase diagram.

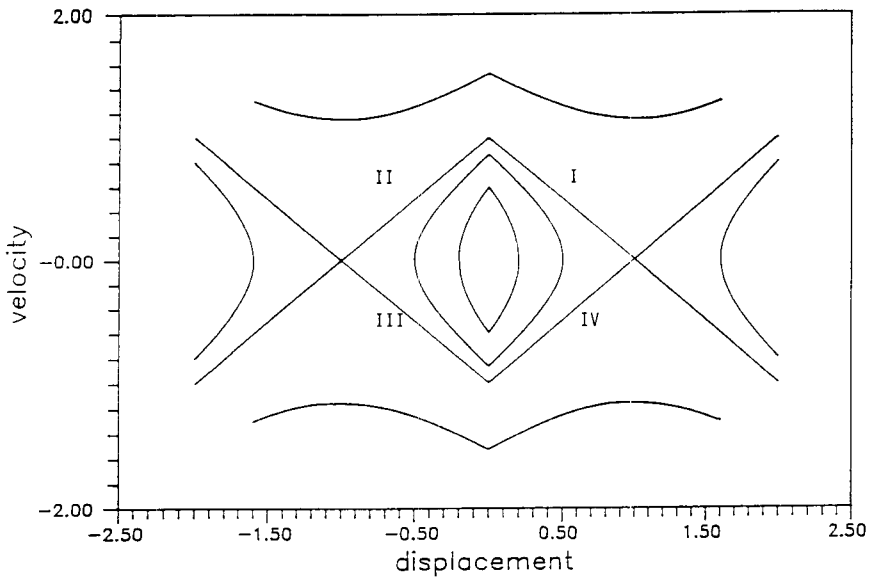

Figure 9.5. Heteroclinic orbit for rocking system.

First the equation of motion is rewritten in the following vector form:

$$\dot{x} = f(x) + \varepsilon g(x,t), \qquad x = (u \quad v)^* \tag{9.6}$$

where the asterisk indicates the transpose of vector (u, v). It is assumed that the unperturbed (i.e., undamped and unforced) system has a Hamiltonian H with $f_1 = \partial H/\partial u$ and $f_2 = \partial H/\partial v$, and the system satisfies the conditions [2] for the existence of two heteroclinic orbits connecting the two unstable hyperbolic singular points forming a closed curve. For the rocking system, it can be shown that these conditions are satisfied. The singular points for the rocking object are unstable equilibrium positions, $(1, 0)$ and $(-1, 0)$, where it stands on one edge (Figure 9.5). In the center of the closed curve is a stable singular point $(0, 0)$. Phase space trajectories near the stable singular point remain in its neighborhood, whereas trajectories near the hyperbolic singular points will diverge from them.

The external force and damping are then represented as perturbations to the Hamiltonian system. The damping effect in the rocking system, which causes sudden reduction in velocity by a factor e at displacement equal to 0, can be expressed analytically by a function $F(\theta, \dot{\theta})$. The integral of this function along the heteroclinic orbit is equal to the energy loss caused by impact in each oscillation. For the rocking system considered, the equation of motion for the general case with damping can be written as

$$I_O\ddot{\theta} \pm MgR(\theta_{cr} \mp \theta) = -MRa_{gx}(t) + F(\theta, \dot{\theta}) \tag{9.7}$$

where $a_{gx} = \varepsilon g \cos \omega t$ is the perturbation caused by external force, and the equation with the upper signs represents equation of motion for $\theta > 0$ and the lower signs for $\theta < 0$. The perturbation due to damping is found to be

$$F(\theta, \dot{\theta}) = -\frac{1}{2} I_O \dot{\theta}^2 (1 - e^2) \left[\delta\left(\frac{\theta}{\theta_{cr}} \right) \right] \left(\frac{1}{\theta_{cr}} \right) \tag{9.8}$$

where $\delta(\theta/\theta_{cr})$ represents the Dirac delta function.

The equation of motion is then rewritten in the format used in (9.6) in the form of a first-order system as follows:

$$\dot{\theta} = v \tag{9.9a}$$

$$\dot{v} = \mp \frac{MgR}{I_O} (\theta_{cr} \mp \theta) - \frac{MgR}{I_O} \varepsilon \cos \omega t - \frac{1}{2} v^2 (1 - e^2) \delta\left(\frac{\theta}{\theta_{cr}} \right) \left(\frac{1}{\theta_{cr}} \right) \tag{9.9b}$$

The Hamiltonian function corresponding to the undamped, unforced system is then found by energy considerations:

$$H(\theta, v) = \frac{v^2}{2} - \frac{MgR}{2I_O} \theta^2 \pm \frac{MgR}{I_O} \theta \theta_{cr} \tag{9.10}$$

If the value of the Hamiltonian, which corresponds to the total (kinetic plus potential) energy of the system, exceeds a critical value ($MgR\theta_{cr}^2/2I_O$), the response will become unbounded, leading to overturning. Conversely, if the total energy is less than the critical value, the response will be bounded and stable.

Next, analytical expressions of the heteroclinic orbits are determined. By equating the Hamiltonian $H(\theta, v)$ and the critical value $MgR\theta_{cr}^2/2I_O$, the heteroclinic orbits can be expressed as functions of time. As mentioned previously, there are two heteroclinic orbits. Note that there is a discontinuity within each heteroclinic orbit and, therefore, four analytical expressions are required to describe the closed curve.

Section I (with $\theta > 0$ and $v > 0$) of the heteroclinic orbit can be expressed as

$$(\theta, v)^1 = (\theta_{cr} - e^{-p}, \alpha e^{-p}) \tag{9.11a}$$

where $p = \alpha t - \ln \theta_{cr}$. Similarly, section II (with $\theta < 0$ and $v > 0$) can be expressed as

$$(\theta, v)^2 = (e^p - \theta_{cr}, \alpha e^p) \tag{9.11b}$$

The expressions of the lower orbit (sections III and IV) can be obtained from (9.11a) and (9.11b) with opposite signs by symmetry. These expressions are then normalized by setting $\Theta = \theta/\theta_{cr}$, $\alpha t = \tau$, $V = v/\theta_{cr}$, and $\omega = \alpha\Omega$, and are rewritten as

$$(\Theta, V)^1 = (1 - e^{-\tau}, e^{-\tau}) \tag{9.12a}$$

$$(\Theta, V)^2 = (e^{\tau} - 1, e^{\tau}) \tag{9.12b}$$

$M^+(t_O)$ is used to denote the Melnikov's function for the upper orbit, and is defined by

$$\begin{aligned} M^+(t_O) &= \int_{-\infty}^{+\infty} f(q_O(t)) \wedge g(q_O(t), t + t_O)\, dt \\ &= \int_{-\infty}^{+\infty} (f_1 f_2) \wedge (g_1 g_2)^*\, dt \\ &= \int_{-\infty}^{+\infty} (f_1 g_2 - f_2 g_1)\, dt \end{aligned} \tag{9.13}$$

where the asterisk represents the transpose of a vector, and the f_is are the linearized Hamiltonians and the g_is are the perturbations. By symmetry, the expressions for $M^-(t_O)$ and $M^+(t_O)$ are identical. Therefore, the existence of solution to $M^+(t_O) = 0$ implies the existence of zero solution to $M^-(t_O)$. Hence, the condition for existence of chaotic response can be determined by examining just the upper curve. When no zeros exist, there is no chaotic response for this system.

The analytical methods for existence and stability of periodic response and the conditions for existence of chaotic response derived previously are applied to the undamped and damped systems in the following sections.

9.5.1. Undamped Systems

The Melnikov function for an undamped slender system can be obtained by letting $F(\theta, v) = 0$, thus (9.13) becomes

$$\begin{aligned} M^+(t_O) &= \frac{-2\varepsilon\alpha^2 \cos \omega t_O}{\theta_{cr}(\alpha^2 + \omega^2)} \\ &= -2A_x \frac{\cos \Omega\tau_O}{1 + \Omega^2} \end{aligned} \tag{9.14}$$

where A_x and Ω are the normalized amplitude and frequency of excitation, respectively, with $A_x = \varepsilon/\theta_{cr}$ and $\Omega = \omega/\alpha$. The zero solutions, which yield the condition for the existence of chaotic response, are given by $\cos \Omega\tau_O = 0$. Because this condition can always be satisfied by $\tau_O = 2n\pi$ for all integer n,

the condition for existence of chaotic response is satisfied by any arbitrary combination of system and excitation parameters.

9.5.2. Damped Systems

For damped systems, the Melnikov function (9.13) can be written as

$$M^+(t_O) = \int_{-\infty}^{+\infty} v^{(2)}(t)\left(\varepsilon\alpha^2 \cos \omega(t + t_O) - F(\theta, \dot{\theta})\right) dt + \int_{-\infty}^{+\infty} v^{(1)}(t)\left(\varepsilon\alpha^2 \cos \omega(t + t_O) - F(\theta, \dot{\theta})\right) dt = \frac{-2\varepsilon\alpha^2 \cos \omega t_O}{\alpha^2 + \omega^2} - \frac{\theta_{cr}(1 - e^2)}{2} \tag{9.15}$$

$M^+(t_O)$ equal to zero is equivalent to

$$\cos \Omega\tau_O = -\frac{(1 - e^2)(1 + \Omega^2)}{4A_x} \tag{9.16}$$

where A_x and Ω are the normalized amplitude and frequency of excitation respectively with $A_x = \varepsilon/\theta_{cr}$ and $\Omega = \omega/\alpha$.

Equation (9.16) can always be satisfied by some τ_O if and only if the magnitude of the right-hand side is less than or equal to unity. Thus, the existence of chaotic response is given by the combination of system parameters e, Ω, and A_x that satisfies the following inequality:

$$\frac{(1 - e^2)(1 + \Omega^2)}{4A_x} \leq 1 \tag{9.17}$$

It can be shown that (9.17) yields only the lower bound for existence of chaotic responses. In the given region, periodic and quasiperiodic responses coexist with chaotic responses [14].

9.6. STOCHASTIC CHARACTERISTICS

When a nonlinear dynamical system is in a chaotic state, precise prediction of the time history of the motion is impractical because small uncertainties in the initial conditions lead to diverging responses. However, probability density functions can provide a statistical measure of the chaotic dynamics. There is some mathematical and experimental evidence that such distributions do exist for chaotic responses [6]. Accordingly, an identification technique for chaotic response in a probabilistic setting, the amplitude probability density function, will be introduced.

Furthermore, in the probabilistic sense, under an almost unique set of initial conditions and a deterministic harmonic steady-state excitation, chaotic responses for certain deterministic structural systems are found to be stochastic [12]. Thus the chaotic process may serve well as a link between the traditional deterministic and stochastic processes. Two stochastic properties of chaotic responses—stationarity and ergodicity—also will be examined.

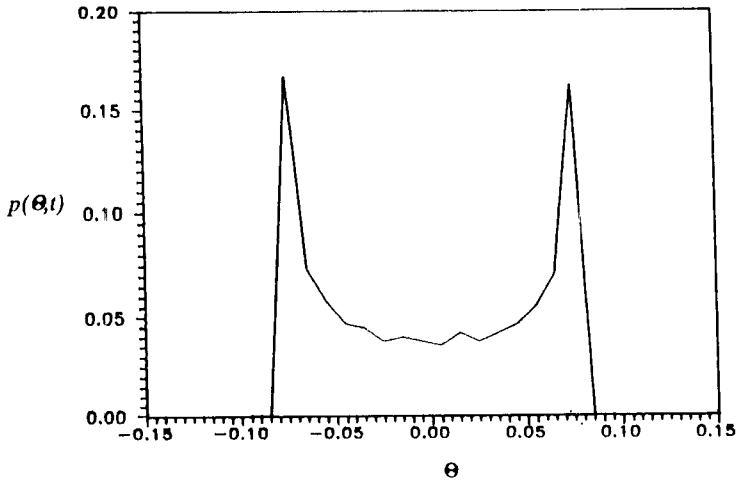

(a)

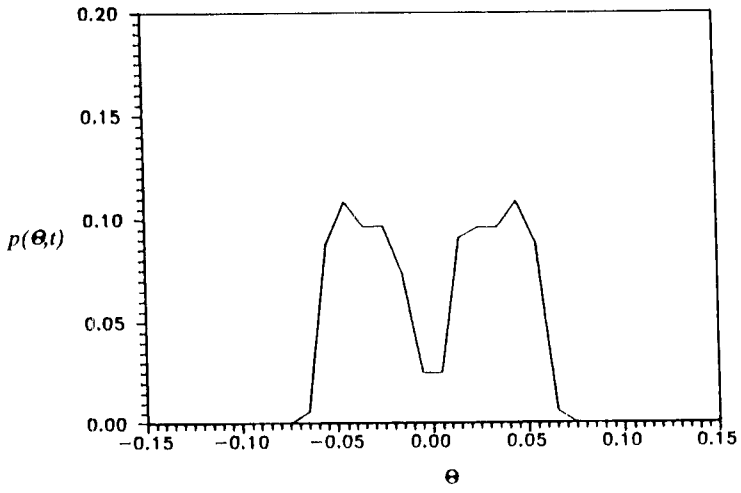

(b)

Figure 9.6. Amplitude probability density functions for periodic responses: (*a*) harmonic response, $A_x = 2.0$ and $T_x = 1.0$; (*b*) one-third subharmonic response, $A_x = 6.5$ and $T_x = 0.4$. ($H/B = 10$, $R = 290$, and $e = 0.925$.)

9.6.1. Amplitude Probability Density Function

The amplitude probability function of a response time history $\Theta(t)$ is defined as the normalized relative frequency of occurrence of the values between Θ and $\Theta + d\Theta$ (i.e., a normalized temporal average of Θ). This definition

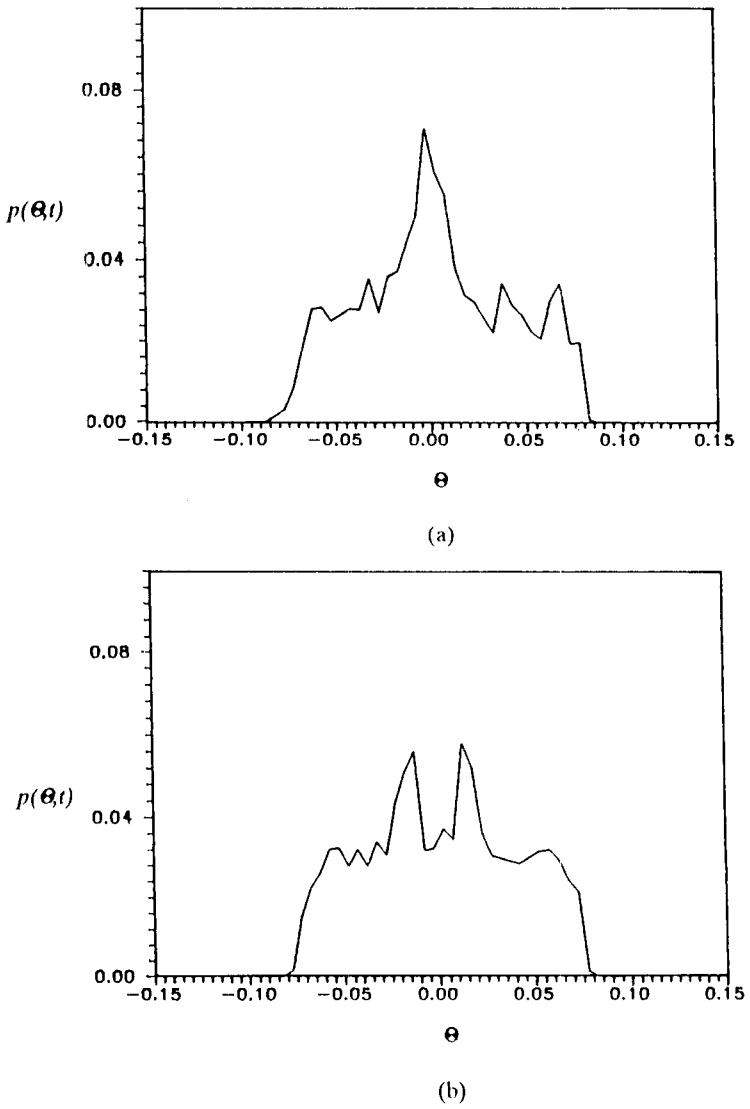

Figure 9.7. Amplitude probability density functions for nonperiodic responses: (*a*) chaotic response, $A_x = 3.0$ and $T_x = 0.4$; (*b*) quasiperiodic response, $A_x = 4.0$ and $T_x = 0.4$. ($H/B = 10$, $R = 290$, and $e = 1.0$.)

differs from the conventional definition of probability density function of $\Theta(t)$ for a given time t in stochastic analysis, which is a normalized ensemble average of the responses falling between Θ and $\Theta + d\Theta$ at time t.

The amplitude probability density functions of a harmonic response and a subharmonic response are shown in Figure 9.6*a* and 9.6*b*, respectively. They are characterized by symmetric maxima at the two extreme values. The maxima diffuse toward the center as the order of the subharmonic response increases.

However, for chaotic responses, the amplitude probability density function is characterized by a multimaxima curve [5], as shown in Figure 9.7*a*. The multimaxima nature of the density function is due to the fact that in the oscillatory waveform of chaotic responses there exist values of the amplitude that are more probable than neighboring values. Although a multimaxima probability density curve is useful in identifying possible chaotic responses, it is not a sufficient indicator. In particular, it cannot differentiate between quasiperiodic and chaotic responses. As shown in Figure 9.7*b*, quasiperiodic response can also have a multimaxima curve in the amplitude probability density function.

9.6.2. Stochastic Properties of Chaotic Response

Stochastic properties for some chaotic systems are known to exist based on "ensemble experiment" [12]. To identify possible stochastic properties of the rocking systems, time histories and Poincaré maps of their chaotic responses are examined. The focus will be on two fundamental properties, stationarity and ergodicity.

Prior to examining the stationarity and ergodicity properties of chaotic responses, it is essential to determine the required sample length of a chaotic time history to ensure stable probability properties. For this we examine the amplitude probability function of a typical chaotic response. To avoid the effects of transience, the response corresponding to the first 3000 cycles of excitation period was discarded. Different segments of the same time history were then sampled. Two representative amplitude probability density functions, each segment equal to 1000 times the excitation period, are shown in Figure 9.8*a* and 9.8*b*. As indicated, the amplitude probability density functions are practically identical, indicating that the segment length is sufficient for convergence of the amplitude probability density function.

A *chaotic process* is defined as an ensemble of chaotic responses that have identical system parameters, but with infinitesimally small perturbations in the initial conditions about a known chaotic attractor, and each sample response is itself chaotic. Numerically, ensembles of responses are generated by computing the time histories of responses of the system with initial conditions corresponding to the grid points of an infinitesimal neighborhood containing the known chaotic attractors. The reference time t is chosen far enough from the initial time that the correlations between each pair of

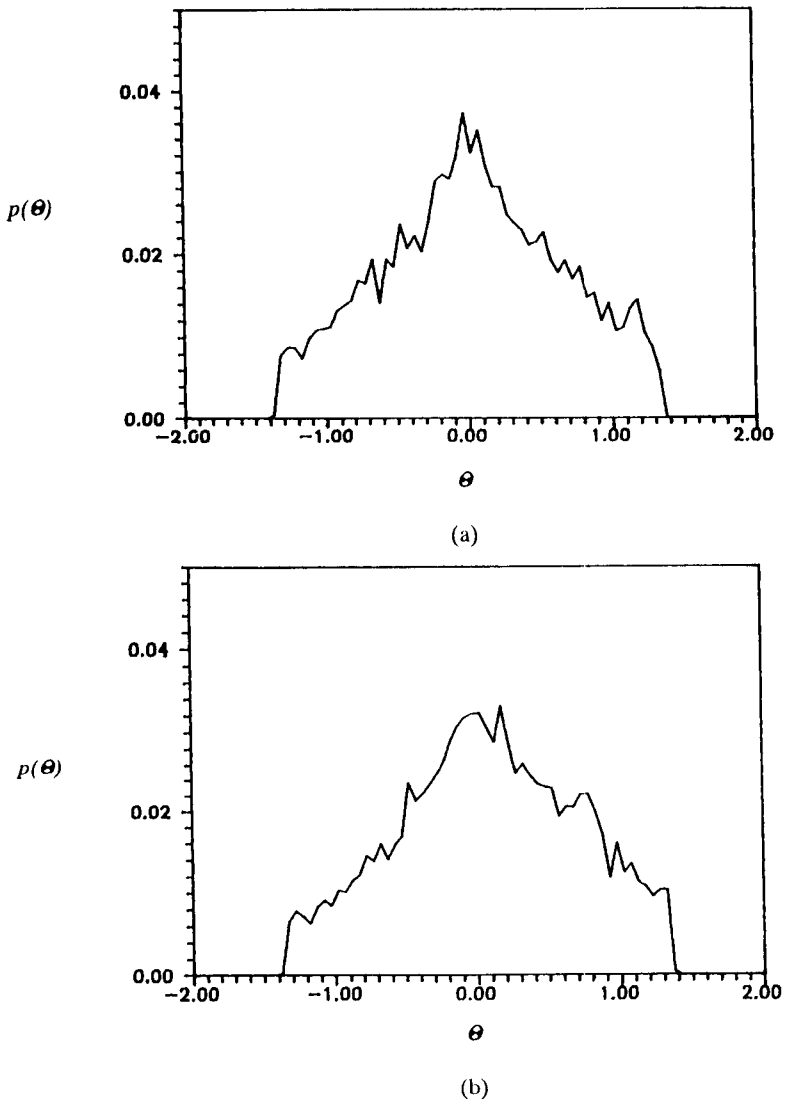

Figure 9.8. Convergence of amplitude probability density functions of chaotic process: (*a*) density function of first 1000-excitation-cycle segment of a chaotic time history; (*b*) density function of second 1000-excitation-cycle segment of the same time history. ($A_x = 4.6$, $T_x = 2.327$, $H/B = 100$, $R = 290$, and $e = 0.5$.)

responses have vanished. In this study, time histories and Poincaré points are generated by computing approximately 1000 time series with initial conditions corresponding to the grid points of a small square. The sizes of the squares are carefully chosen to ensure the samples are representative of the chaotic processes.

Time History. A stochastic process $\Theta(t)$ is stationary if its statistical properties are invariant to a shift of the time reference, that is, the process $\Theta(t)$ and $\Theta(t + \phi)$ have identical distributions for any value of ϕ. To test stationarity

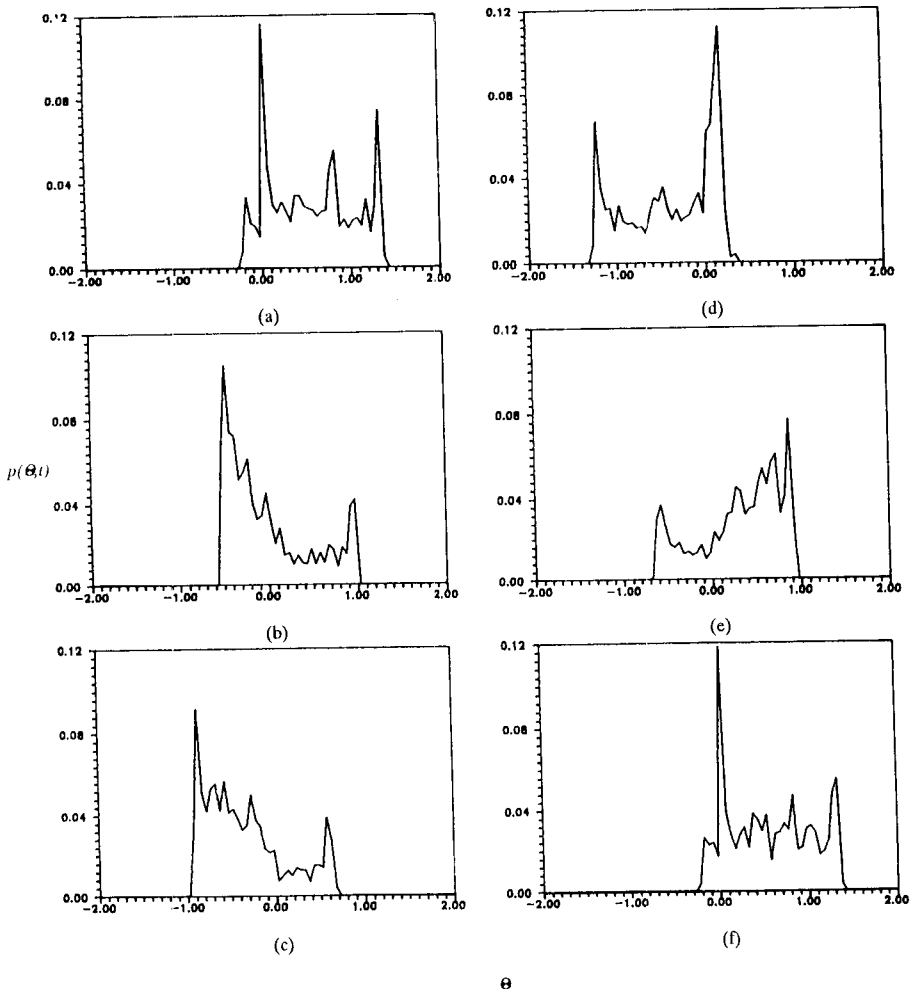

Figure 9.9. Probability density functions with sampling shifts (ϕ): (*a*) $\phi = 0.0 \times T_x$; (*b*) $\phi = 0.2 \times T_x$; (*c*) $\phi = 0.4 \times T_x$; (*d*) $\phi = 0.6 \times T_x$; (*e*) $\phi = 0.8 \times T_x$; (*f*) $\phi = 1.0 \times T_x$. ($A_x = 4.6$, $T_x = 2.327$, $H/B = 100$, $R = 290$, and $e = 0.5$.)

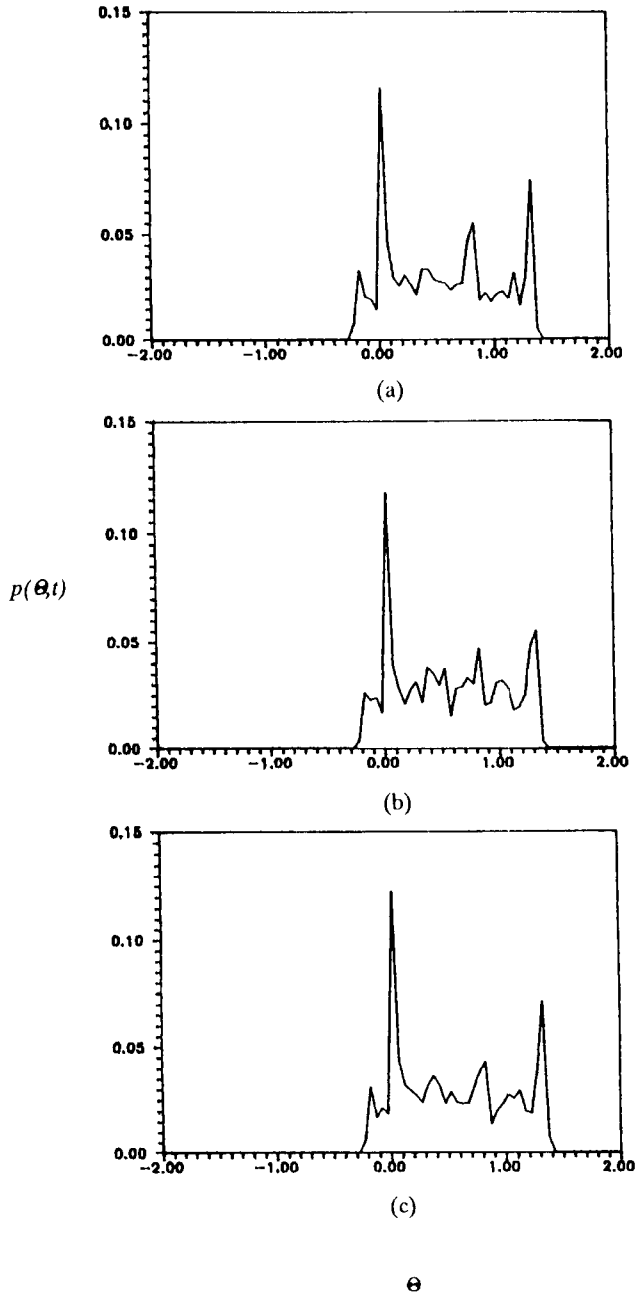

Figure 9.10. Stationarity and ergodicity of Poincaré time series: (*a*) probability density function at $t = 100T$; (*b*) probability density function at $t = 150T$; (*c*) amplitude probability density function of a typical time series. ($A_x = 4.6$, $T_x = 2.327$, $H/B = 100$, $R = 290$, and $e = 0.5$.)

of chaotic responses, the probability density functions of a (5000-sample) chaotic process corresponding to six values of time shifts (ϕ = 0.0, 0.2, 0.4, 0.6, 0.8, and 1.0 times the excitation period) are presented in Figure 9.9. The time t is chosen as the end of the 1000th cycle of the excitation. Note that the probability density function is dependent on the phase shift; thus chaotic time histories are nonstationary. However, when the phase shift is an integer multiple of the excitation period, the probability density functions are nearly identical (Figures 9.9*a* and 9.9*f*). In addition, the probability density function appears to be symmetric about the half-cycle time point, that is, the function at 0.4 and 0.6 (Figure 9.9*c* and 9.9*d*) and the function at 0.2 and 0.8 (Figure 9.9*b* and 9.9*e*) are practically equal. Thus the time dependence appears to be periodic with period equal to the excitation period, and there may be an invariant structure when periodic dependency is removed.

Poincaré Maps. The Poincaré points generated from the 1000-sample time histories may themselves be considered as time series with a sampling rate equal to the excitation period. The probability density functions at two representative times t_1 and t_2 of the Poincaré time series of a chaotic process are shown in Figure 9.10*a* and 9.10*b*. It is observed that the two functions are practically identical, thus indicating that the Poincaré processes of chaotic responses are stationary. This property is anticipated because the trajectory of chaotic response settles into a strange attractor; hence, after transient response has died out, the shape of the Poincaré map will not change with time.

Yang and Cheng [12] observed an interesting behavior of the Poincaré points of chaotic responses. In their study of nonlinear structures with hysteresis and degradation, they found that the asymptotic distribution of the Poincaré points originating from the infinitesimal square appear to be identical to that of the Poincaré map of a single time history. In particular, for small multiples of the excitation period T, the Poincaré points stay close together. As time increases, the Poincaré points keep stretching and folding (Smale horseshoe effect [8]). Eventually, the Poincaré points settle down into the same attractor as the one created by a single time history. This phenomenon is demonstrated in Figure 9.11 for the chaotic rocking responses. Numerical results indicate that the convergent rate of ergodicity depends on the chosen small square of initial conditions and the system sensitivity. If the small square of initial conditions falls in the sensitive region of the chaotic state, the strange attractor can be achieved by fewer loading cycles. Furthermore, the more sensitive the response is, the fewer loading cycles are needed for the ensemble Poincaré points to reach the distribution of the strange attractor. Thus the rate of convergence of the Poincaré process to the chaotic attractor may also be used as a measure of the sensitivity of the system response.

Poincaré processes of the rocking systems are further examined for ergodicity in this study by examining the probability density functions. A stochastic

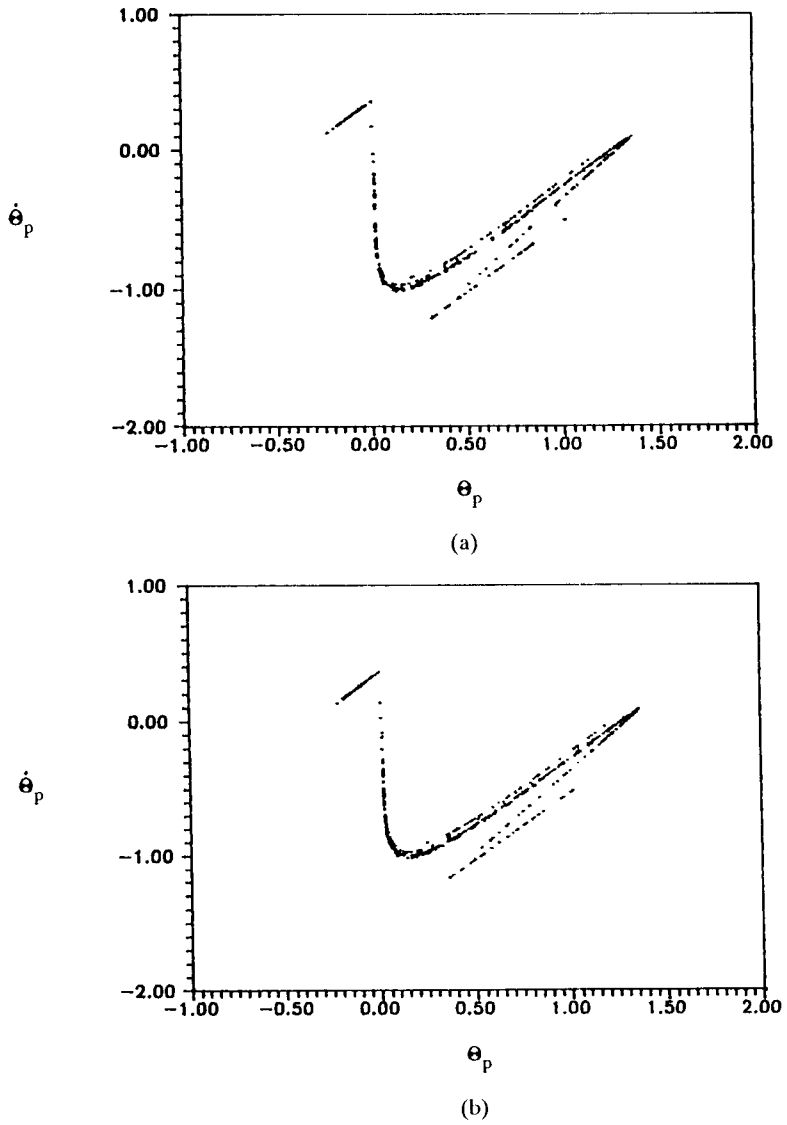

Figure 9.11. Ergodicity in terms of Poincaré time series: (*a*) ensemble time series; (*b*) one time history. ($A_x = 4.6$, $T_x = 2.327$, $H/B = 100$, $R = 290$, and $e = 0.5$.)

process $\Theta(t)$ is ergodic if its ensemble average equals appropriate time average, that is, with probability 1, the statistics of $\Theta(t)$ can be determined from a single sample $\Theta(t, \zeta)$. To examine the ergodic property of the Poincaré process, the amplitude probability density function constructed from a single time series (Figure 9.10*c*) is compared to those obtained from the 1000 sample Poincaré process discussed (Figure 9.10*a* and 9.10*b*). Ob-

serve that the two types of distributions are practically identical, which indicates that the Poincaré process may be ergodic. The properties of the correlation function of the Poincaré process will be examined in detail in a future paper to confirm ergodicity.

9.7. CONCLUSIONS

This investigation deals with the identification of stochastic properties of chaotic response of a dynamical system describing the rocking response of rigid objects to horizontal harmonic base excitation. The existence periodic, chaotic, and quasiperiodic responses are demonstrated. An analytical technique based on the Melnikov function is derived for the prediction of existence of chaotic response. The stochastic dynamics of the rocking system are examined by merging and extending the numerical analysis techniques developed by Kapitaniak [5] and Yang and Cheng [12]. It is found that in a stochastic sense, probability density functions are time dependent; hence, a process formed by time histories of chaotic responses is not stationary. However, a process consisting of Poincaré points of chaotic responses as time histories may be ergodic. These stochastic properties are useful for fatigue design of nonlinear dynamical systems with frequent chaotic motions.

Finally, the excitations considered in this study are purely deterministic. For future research, it would be interesting to apply the stochastic techniques to examine the behavior of nonlinear dynamical systems subjected to excitations with significant stochastic components.

ACKNOWLEDGMENT

The authors gratefully acknowledge the financial support for this research by the Office of Naval Research Young-Investigator Award under Grant No. N00014-88-K-0729.

NOTATION

a_{gx}, a_{gy}	horizontal and vertical ground accelerations
a_x, a_y	amplitude of horizontal and vertical excitations
a_s	coefficient of periodic steady-state response
A_x	normalized amplitude of horizontal excitation, $A_x = a_x/(g\theta_{cr})$
A_y	normalized amplitude of horizontal excitation, $A_y = a_y/g$
b_s	coefficient of periodic steady-state response
d_c	fractal dimension
e	coefficient of restitution
g	acceleration of gravity

r_a	ratio of vertical versus horizontal excitation amplitude, $r_a = a_y/a_x$
B, H	width and height of block
I_O	mass moment of inertia
M	mass of object
$p(\Theta, t)$	amplitude probability density function
R	radius of rotation
T_x	period of horizontal excitation
θ	rotation of angle of rocking block
θ_b	bracing angle
θ_{cr}	critical angle
$\dot{\theta}$	angular velocity
Θ	normalized angle, $\Theta = \theta/\theta_{\text{cr}}$
$\dot{\Theta}$	normalized angular velocity, $\dot{\Theta} = \dot{\theta}/\theta_{\text{cr}}$
α	$(MgR/I_O)^{1/2}$
β	$A_x/(1 + \Omega^2)$
τ	initial time, $\tau = \alpha t$
τ_i	the instant of occurrence of impact
Ω	normalized frequency of horizontal excitation
λ	Lyapunov exponent
ω_x	frequency of horizontal excitation
ϕ	sampling shift
ϕ_s	shift between excitation and steady-state response

REFERENCES

1. M. Aslam, W. G. Godden, and D. T. Scalise, Earthquake rocking response of rigid bodies. *J. Structural Eng. Div. ASCE* **106** (ST2) 377–392 (1980).
2. J. Guckenheimer and P. Holmes, *Nonlinear Oscillations, Dynamical Systems, and Bifurcations of Vector Fields*. Springer-Verlag, New York, 1983.
3. S. J. Hogan, On the dynamics of rigid-block motion under harmonic forcing. *Proc. Roy. Soc. London A* **425** 441–476 (1989).
4. S. J. Hogan, The many steady state responses of a rigid block under harmonic forcing. *Earthquake Eng. and Structural Dynam.* **19** 1057–1071 (1990).
5. T. Kapitaniak, Quantifying chaos with amplitude probability density function. *J. Sound and Vibrations* **114** 588–592 (1987).
6. F. C. Moon, *Chaotic Vibrations*. Wiley, New York, 1987.
7. P. D. Spanos and A. S. Koh, Rocking of rigid blocks due to harmonic shaking. *J. Eng. Mech. Div. ASCE* **110** 1627–1642 (1984).
8. J. M. T. Thompson and H. B. Stewart, *Nonlinear Dynamics and Chaos*. Wiley, New York, 1986.
9. W. K. Tso and C. M. Wong, Steady state rocking response of rigid blocks, Part I: Analysis. *Earthquake Eng. and Structural Dynam.* **18**(106) 89–106 (1989).

10. A. Wolf, J. B. Swift, H. L. Swinney, and J. A. Vastano, Determining Lyapunov exponent from a time series. *Physica D* **16** 285–317 (1985).
11. C. M. Wong and W. K. Tso, Steady state rocking response of rigid blocks, Part II: Experiment. *Earthquake Eng. and Structural Dynam.* **18**(106) 107–120 (1989).
12. C. Y. Yang, A. H-D. Cheng, and R. V. Roy, Chaotic and stochastic dynamics for a nonlinear structural system with hysteresis and degradation. *Int. J. Probabilistic Eng. Mech.* **6**(3/4) 193–203 (1991).
13. C. S. Yim, A. K. Chopra, and J. Penzien, Rocking response of rigid blocks to earthquakes. *Earthquake Eng. and Structural Dynam.* **8**(6) 565–587 (1980).
14. S. C. S. Yim and H. Lin, Chaotic behavior and stability of free-standing offshore equipment. *Ocean Eng.* **18**(3) 225–250 (1991).